

Short-time scales in the Kramers problem: past, present, future (review and roadmap dedicated to the 95th birthday of Emmanuel Rashba)

Stanislav M. Soskin^{1,*} and Tetiana L. Linnik^{1,2,†}

¹*Institute of Semiconductor Physics, National Academy of Sciences of Ukraine, 03680 Kyiv, Ukraine*

²*Experimentelle Physik 2, Technische Universität Dortmund, 44227 Dortmund, Germany*

(Dated: January 30, 2023)

The problem of noise-induced transitions is often associated with Hendrik *Kramers* due to his seminal paper of 1940, where an archetypal example - one-dimensional potential system subject to linear damping and weak white noise - was considered and the quasi-stationary rate of escape over a potential barrier was estimated for the ranges of extremely small and moderate-to-large damping. The gap between these ranges was covered in the 80th by one of Rashba's favourite disciples Vladimir Ivanovich Mel'nikov.

It is natural to pose a question: *how does the escape rate achieve the quasi-stationary stage?* At least in case of a single potential barrier, the answer seems to be obvious: the escape rate should smoothly and monotonously grow from zero at the initial instant to the quasi-stationary value at time-scales of the order of the time required for the formation of the quasi-stationary distribution within the potential well. Such answer appeared to be confirmed by the analytic work of Vitaly Shneidman in 1997. However our works in the end of the 90th and in the beginning of the 2000th in collaboration with one more Rashba's favorite disciple Valentin Ivanovich Sheka and with Riccardo Mannella showed that, at a shorter time-scale, namely that of the order of the period of natural oscillations in the potential well, the escape rate growth generically occurred *stepwise* or even in an oscillatory manner. Analytic results were confirmed with computer simulations.

In the *present paper*, we review those results and provide a roadmap for the development of the subject, in particular demonstrating that various recently exploited experimental systems are excellent candidates for the observation of the above non-trivial theoretical predictions and, moreover, they promise useful applications.

PACS numbers: 05.40.-a, 05.10.Gg, 02.70.Lq

I. RASHBA'S INFLUENCE ON OUR LIVES

Prior to the passing to a purely scientific part of the paper, we would like to do an informal introduction dedicated to Emmanuil Iosifovich Rashba (to whom, for the sake of brevity, we further refer as EIR) and to tell about his role in our life. SMS tells as follows.

"I have been knowing EIR for about 57 years. In 1965, when I was about five-years old, our family moved to a house 103/3 at Bolshaya Kitaevskaya street in Kiev. EIR lived in a neighbouring section of the same house and I met him sometimes in the yard. My father said to me: "This man is an outstanding physicist-theoretician!" I was however more interested in his daughter Yulia. Being about my age, she was beautiful, smart, and amiable. I liked playing with her in the yard of our house. Regrettably for me, the communication with Yulia stopped rather soon: in 1966, her father accepted an offer to head the Theory of Semiconductors Division at the recently founded Institute of Theoretical Physics in Chernogolovka and moved there together with the family.

My next (implicit) intersection with EIR occurred as a meeting with his scientific "child", namely one of his favourite disciples Vladimir Ivanovich Mel'nikov, who followed the mentor in his moving from Kiev to Chernogolovka. I was introduced to Mel'nikov by my mentor Mark Isaakovich Dykman in 1986 in Moscow at

the General Meeting of the Academy of Sciences of USSR devoted to the discovery of the high-temperature superconductivity. My mentor asked Mel'nikov to be the primary referee of my thesis for the candidate of sciences degree (the PhD analogue). Mel'nikov agreed. Allowing for that, I decided to study his papers in order to properly cite them in the thesis. I found then that he had done an extraordinarily beautiful work [1, 2] (see [3] for review and more references) on the matching between strongly underdamped and moderate-to-large-damping limits in the Kramers problem of the quasi-stationary escape from a potential well induced with a weak white noise [4] (this problem laid unsolved for more than 40 years despite numerous attempts of its solution [3]).

Although I never used immediate results of Mel'nikov's work, it played an important role in my scientific life. Indeed, I used one of the auxiliary ideas exploited by Mel'nikov in his work, namely the idea to use a Gaussian distribution with an increasing in time width in certain integral equation. This helped me to obtain a semi-explicit solution of a problem completely different from the Kramers problem, namely to find a universal shape of characteristic peaks in fluctuation spectra of a broad class of systems, which inherently required to find a non-trivial dynamics of a system in contrast to the quasi-stationary distributions considered by Mel'nikov. When I showed the semi-explicit results to my mentor, he sug-

gested that these results indicated that, the corresponding non-stationary Fokker-Planck equation (FPE) for the probability density could be reduced to some universal equation and might be it would be possible to solve it. His keen intuition turned out right: in the relevant underdamped asymptotic limit, I reduced the complicated general form of the FPE to a relatively simple but still non-trivial equation in partial derivatives of the 2nd order and, even more important, managed to find its explicit solution, which allowed me in turn to find the universal shape of spectral peaks in such a class of systems. I consider this work [5] as one of my best ones. Moreover, it have played the major role in an identification of certain variety of fluctuational and dynamical phenomena as a characteristic class of the so called zero-dispersion phenomena (see [6–8] and references therein).

Not only was I glad to have solved the important physical problem in [5] but I was also proud with the fact that I was seemingly the first person who had solved this non-trivial differential equation in partial derivatives of the 2nd order. When I worked on some quantum problem a few years afterwards, I was studying the book “Statistical Mechanics” by Feynman [9] and found there ... almost the same equation in a completely different physical context! The problem where it arose in studies by Feynman was a problem about the stationary density matrix in a harmonic oscillator: the variables of the properly normalized reciprocal temperature and coordinate in Feynman’s problem corresponded accordingly to the variables of the properly normalized time and energy in my problem. The only difference between the normalized equations was that the multiplier of the nontrivial (quadratic) term in Feynman’s equation was purely real while that in mine was purely imaginary. Correspondingly, the structure of the solution from the physical point of view strongly differed while the mathematical one was the same. The way in which Feynman obtained the solution was exactly the same as I did. He was apparently so excited with the beauty of this way that, similarly to me, presented it in full detail. I was disappointed by the fact that the priority in the solution of the mathematical equation was not mine, but the disappointment was decreased due to a feeling that I had something in common with such an outstanding scientist as Richard Feynman. In order to transform this thrilling story into the closed loop, I need to add the following. Mentors of Mel’nikov and Dykman (whose ideas inspired me, as demonstrated above) were EIR and Mikhail Alexandrovich Krivoglaz respectively while both Rashba and Krivoglaz had one and the same mentor - Solomon Isaakovich Pekar; and the loop is being closed as follows: in the famous book “Quantum Mechanics and Path Integrals” [10], Feynman refers only to 26 sources (a very small amount as for a book, which means that only truly fundamental sources were referred) and 2 of these sources were papers by Pekar! The story on the whole demonstrates amazing links threading the

world in terms of science, geography, time (generations), and, in a sense, noosphere.

My next implicit intersection with EIR occurred via collaboration with another his favourite disciple - Valentin Ivanovich Sheka - and Sheka’s disciple Tat’yana Leontievna Linnik. The most exciting results of this collaboration will be presented in the next sections. So, I do not go in details here. Rather I just mention that the collaboration lasted since 1999 till 2005 and resulted in 11 papers (most important of which are [11–17]) and, in addition, stimulated 1 more my paper without coauthors [18]. The collaboration could last more but Sheka’s health problems and my intensive involvement in other projects had led to its interruption.

It turned out that EIR followed my joint activity with Sheka, and we communicated with him a few times via email on this and other occasions. The most active communication was in July 2021, when I organized the ZOOM seminar dedicated to the memory of V.I. Sheka who died of coronavirus on the 7th of February 2021. EIR was a key speaker at the seminar, and I enjoyed both a communication with him on the eve of the seminar and, yet more so, listening to his lecture (lasting almost an hour!) about the development of theoretical physics in Kiev in the 40th-50th of the previous century, the seminal joint paper with Sheka [19], the current state of art and perspectives of spintronics.

In one of the letters to my father (with whom EIR was in friendly relations for more than 60 years until the very death of my father in 2020), EIR wrote: “The greatest present which one could get in old age is a clear mind.” *EIR has been lucky to get such a present.*”

TLL tells as follows. “Though I did not immediately work with EIR, I did feel his influence through his disciple Valentin Ivanovich Sheka (VIS) who became my mentor and a very close person for me for the thirty years of our communication with each other. I felt the influence of EIR especially strongly during the work on the book [20]. The book was based on the course of lectures presented by VIS at the Physics Department of Kiev State University in the 60th-80th of the previous century and more recently by me. Many works of EIR were immediately used in the book. I was particularly pleased to know about a high evaluation of the book by EIR and, yet more so, to hear in the lecture by EIR at the aforementioned seminar dedicated to the memory of VIS that the book is highly valued by some of Russian-speaking scientists in the USA. In particular, EIR told that Prof. Lev Levitov preferred using just this book for his teaching a similar course in MIT rather than the first book on the subject [21] because our book was much easier for a perception by students and because we illustrated the efficiency of the method of invariants at a few modern systems and materials, for example graphene. Concluding this personal dedication, I would like to say that I am very happy to have such a “scientific grandfather” as

EIR, and I wish him to further keep his love to physics and life on the whole and to inspire younger researchers.”

II. INTRODUCTION TO THE SCIENTIFIC PART

In his seminal work [4], Kramers considered a weak noise-induced flux from a single metastable classical potential well, i.e. he considered a stochastic system

$$\begin{aligned} \ddot{q} + \Gamma \dot{q} + dU/dq &= f(t), \\ \langle f(t) \rangle &= 0, \quad \langle f(t)f(t') \rangle = 2\Gamma T \delta(t-t'), \quad T \ll \Delta U, \end{aligned} \quad (1)$$

which was put initially at the bottom of a metastable potential well $U(q)$ with a barrier ΔU , and he then calculated the quasi-stationary probability flux across the barrier. Models of type (1) are relevant to chemical reactions [4], SQUIDs [22], nano/micro-mechanical resonators (see e.g. [8, 23] and references therein), nano-particles in optical traps [24] and other real systems (see some of the references in [3]).

There have been many developments and generalizations of the Kramers problem but both Kramers and most of those who followed him considered only the *quasi-stationary* flux, i.e. the flux established after the formation of a quasi-equilibrium distribution within the well (up to the barrier). The quasi-stationary flux is characterized by a slow exponential decay in time t , an Arrhenius dependence on temperature T , and a relatively weak dependence on friction Γ :

$$J_{qs}(t) = \alpha_{qs} e^{-\alpha_{qs} t}, \quad \alpha_{qs} = P e^{-\frac{\Delta U}{T}}, \quad (2)$$

where P depends on Γ and T in a non-activated way.

But how does the flux evolve from its zero value at initial time to its quasi-stationary regime (2) at time-scales exceeding the time t_f for the formation of quasi-equilibrium? The answer may obviously depend on initial conditions and a relevant boundary (i.e. the boundary through which the escape occurs). As for the boundary, it can be shown that the most general qualitative features of the flux are valid for any type of boundary (for the sake of simplicity, we shall consider below only the absorbing wall). As for the initial conditions, their relevance may vary. The simplest and often relevant initial state is the bottom of the well, since it is the stable stationary state in the absence of noise: if the noise (not necessarily of the thermal origin) is switched on at some instant, then the time evolution of the escape from the *bottom* becomes relevant. It should be emphasized however that, if the relevant metastable part of the potential is multi-well, then the flux during the major part of the relevant time is not sensitive to the initial state provided it is concentrated just in one well (e.g. it may be thermalized in the well). As for the single-well case, the flux evolution is more sensitive to the initial state and we shall consider various cases. But, first, let us discuss the most

simple case where the initial state is at the bottom of the potential. We shall refer to it as the *bottom initial state*.

It may seem natural to assume that the flux evolution from zero to the quasi-stationary regime is a monotonic function without any “irregularities”. Apart from the naive argument that “noise smooths everything”, this assumption appears sound because the probability distribution W is distinctly centered at the bottom of the well both initially and in the quasi-stationary stage: $W(q, \dot{q}, t=0|q_0=q_b, \dot{q}_0=0) = \delta(q-q_b)\delta(\dot{q})$ while $W(q, \dot{q}, t \gg t_f|q_0=q_b, \dot{q}_0=0)$ is a narrow peak of width $\propto \sqrt{T}$ around that same state $\{q=q_b, \dot{q}=0\}$. Moreover, it was shown in Ref. 24 that, both in the underdamped and overdamped limits, the escape flux $J(t)$ does grow at $t \sim t_f$ in a simple manner.

Despite the above arguments, it can be shown that, generically, J evolves from $J(0)=0$ to $J_{qs}(t \gg t_f)$ in a quite complicated way.

1. As shown in Sec. III.A, the flux grows *step-wise* on time-scales of the order of a *period of eigenoscillation* in the bottom of the well. Apart from a purely theoretical interest in filling the “gap” in time-scales in the Kramers problem, this part of our work [11–16, 18] was motivated by the growing interest in the short time-scales that became relevant in the 90th to some experiments, e.g. those studying chemical reactions down to femtosecond time-scales [26]: the period of eigenoscillations relevant to chemical reactions in Ref. 25 is ~ 1 –100 fs.
2. As shown below in Section III.B, the evolution of the flux on longer time-scales in a *multi-well* metastable potential is also distinctly different from the relatively simple monotonic function described in Ref. 24: J grows sharply on a logarithmic time-scale to a value which is typically very different from $J_{qs}(0)$ (typically, exponentially larger) and then evolves to $J_{qs}(t)$ during the exponentially long time.

It should be emphasized that the qualitative features of $J(t)$ described above are valid for any reasonable definition of the flux: e.g. the full flux through a boundary or just the first-passage flux, while the boundary may be a given coordinate, or a boundary of a basin of attraction, or a boundary of the vicinity of another attractor, etc.

For illustration, we use the potential

$$U(q) = q - q^3/3 \quad (3)$$

for the single-well case (Fig. 1), and

$$U(q) = 0.06(q + 1.5)^2 - \cos(q) \quad (4)$$

for the multi-well case (Fig. 6(a)), with an absorbing wall [27] at $q = q_{aw}$ in both cases. Experimentally, the flux is measured in the following way. The system is placed at an initial state, after which it follows the stochastic equation (1) until either the coordinate of the wall, q_{aw} , or the time limit [28], t_l , is reached. It is then reset to the initial state and everything is repeated. Once the statistics are deemed adequate, we calculate the flux

$$J(t) \equiv \frac{1}{N_{\text{reset}}} \frac{\Delta N(t)}{\Delta t} \quad (5)$$

where N_{reset} is the overall number of resets, and $\Delta N(t)$ is the number of resets during the interval $[t, t + \Delta t]$; Δt is chosen to be much smaller than a characteristic time over which the flux (5) may change significantly, but large enough to provide $\Delta N(t) \gg 1$ (roughly, the latter is satisfied provided $\Delta t \gg t_l/N_{\text{reset}}$).

The above experimental definition corresponds to the following theoretical definition of the flux

$$J(t) = \int \int dq_0 d\dot{q}_0 W_{in}(q_0, \dot{q}_0) J_{q_0, \dot{q}_0}(t), \quad (6)$$

$$J_{q_0, \dot{q}_0}(t) = \int_0^\infty d\dot{q} \dot{q} W(q = q_{aw}, \dot{q}, t | q_0, \dot{q}_0),$$

where $W_{in}(q_0, \dot{q}_0)$ is a statistical distribution of the initial coordinate and velocity and W is the conditional probability density.

The theoretical approach which we use is the method of *optimal fluctuation* (see e.g. Refs. 10 and 28) whose details in application to the present problems are given in the next section. Results of a verification of theoretical results by computer and analog electronic simulations are also presented.

The structure of the rest of the paper is the following. Sec. III gives the review of former results on the subject. The subsections A and B consider the cases of single-well and multi-well potentials respectively. In Sec. IV, we briefly present the roadmap for the most interesting developments of the subject including issues of a scientific and practical interest, in the subjects A and B respectively. Conclusions are given in Sec. V.

III. REVIEW OF FORMER RESULTS

A. Single-well metastable potential

It can be shown directly from the Fokker-Plank equation that the formation of quasi-equilibrium up to the barrier in the single metastable well typically takes [30] a time of the order of

$$t_f^{(s)} \sim \frac{1}{\min(\Gamma, \omega_0^2/\Gamma)} \ln\left(\frac{\Delta U}{T}\right), \quad (7)$$

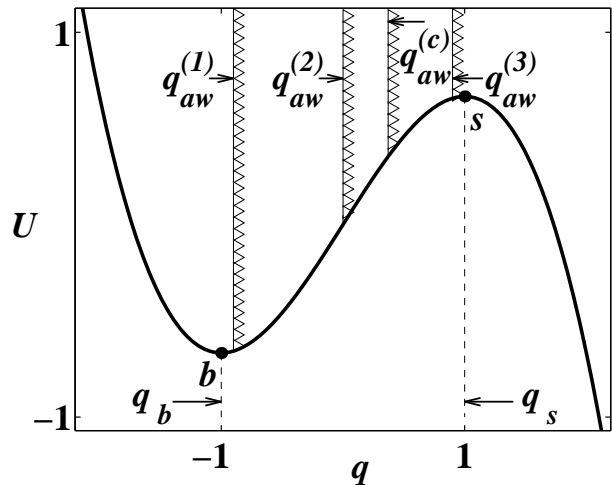


FIG. 1: The potential $U(q) = q - q^3/3$. The bottom and the saddle are marked as b and s respectively. Triangles indicate four typical positions of the absorbing wall.

where ω_0 is the frequency of eigenoscillation in the bottom of the well.

In this section, we shall be interested in much smaller time-scales,

$$t \ll t_f^{(s)}. \quad (8)$$

The work on *non-stationary* escape rates in the Kramers problem preceding to ours was based on the direct solution of the Fokker-Plank equation (cf. [25]). The method of *optimal fluctuation* to this problem was applied for the first time in [32] and then further developed in [11–16, 18], obtaining non-trivial new results for short time-scales. It is convenient to consider first the case of an initial state with a *given* coordinate and velocity:

$$W_{in}(q_0, \dot{q}_0) = \delta(q_0 - q_i) \delta(\dot{q}_0 - \dot{q}_i). \quad (9)$$

The flux is sought as

$$J(t) \equiv J_{q_i, \dot{q}_i}(t) = P(t) e^{-\frac{S_{\min}(t)}{T}} \quad (10)$$

where the *activation energy* $S_{\min}(t)$ does not depend on T while the prefactor $P(t)$ depends on T in a non-activated way. At small T and short t , the factor $\exp(-S_{\min}/T)$ depends on t much more strongly than P . So, we concentrate on studying $S_{\min}(t)$, which can be shown [32] to be a minimum of the functional:

$$S_{\min}(t) \equiv S_{\min}(q_i, \dot{q}_i, t) = \min_{[q(\tau), \dot{q}_{aw}(S)]} (S),$$

$$S \equiv S_{\dot{q}(t)}[q(\tau)] = \int_0^t d\tau L, \quad (11)$$

$$L = (\ddot{q} + \Gamma\dot{q} + dU/dq)^2/(4\Gamma), \quad (12)$$

$$q(0) = q_i, \quad \dot{q}(0) = \dot{q}_i, \quad q(t) = q_{aw}, \quad \dot{q}(t) = \dot{q}_{aw}. \quad (13)$$

The minimization is done over an escape path $[q(\tau)]$ at a given exit velocity \dot{q}_{aw} , with a further minimization over \dot{q}_{aw} [33]. The path minimizing S may be called the *most probable escape path* (MPEP), in analogy with the quasi-stationary case. The necessary conditions for the minimum of the functional (11) are as follows.

1. A zero variation, $\delta S = 0$: it implies that the MPEP $[q(\tau)]$ satisfies the Euler-Poisson equation [32, 36]

$$\frac{\partial L}{\partial q} - \frac{d}{dt} \left(\frac{\partial L}{\partial \dot{q}} \right) + \frac{d^2}{dt^2} \left(\frac{\partial L}{\partial \ddot{q}} \right) = 0, \quad (14)$$

which, for the L of the form (12), reads

$$\ddot{q} + \ddot{q} \left(2 \frac{d^2 U}{dq^2} - \Gamma^2 \right) + \dot{q}^2 \frac{d^3 U}{dq^3} + \frac{d^2 U}{dq^2} \frac{dU}{dq} = 0. \quad (15)$$

2. A zero derivative with respect to the exit velocity, $\partial S / \partial \dot{q}(t) = 0$: this condition can be reduced to $\partial L / \partial \ddot{q}(t) = 0$, which, for the L of the form (12), reads

$$[\ddot{q} + \Gamma\dot{q} + dU/dq]|_{\tau=t} = 0. \quad (16)$$

Solutions of Eq.(15) satisfying three first conditions in (13) and the condition (16) can be found numerically: in addition to $q(0)$ and $\dot{q}(0)$ given in (13), one can match $\ddot{q}(0)$ and $\ddot{q}(t)$ so that the result of the integration (15) on the interval $[0, t]$ satisfies the third condition in Eq. (13) (i.e. $q(t) = q_{aw}$) and the condition (16).

1. Bottom initial state

Let us first consider the case of the bottom initial state:

$$q_i = q_b, \quad \dot{q}_i = 0. \quad (17)$$

Before presenting the numerical results, we find important general features of the MPEPs and $S_{\min}(t)$. In particular, we show below that, as the boundary moves from the close vicinity of the bottom towards the saddle, $J(t)$ undergoes qualitative changes while still being step-wise.

First, consider the case when the absorbing wall is close to the bottom: $U(q)$ may then be approximated by a parabola (Fig.2(a))

$$U(q) - U(q_b) \approx \frac{\omega_0^2}{2} (q - q_b)^2, \quad (18)$$

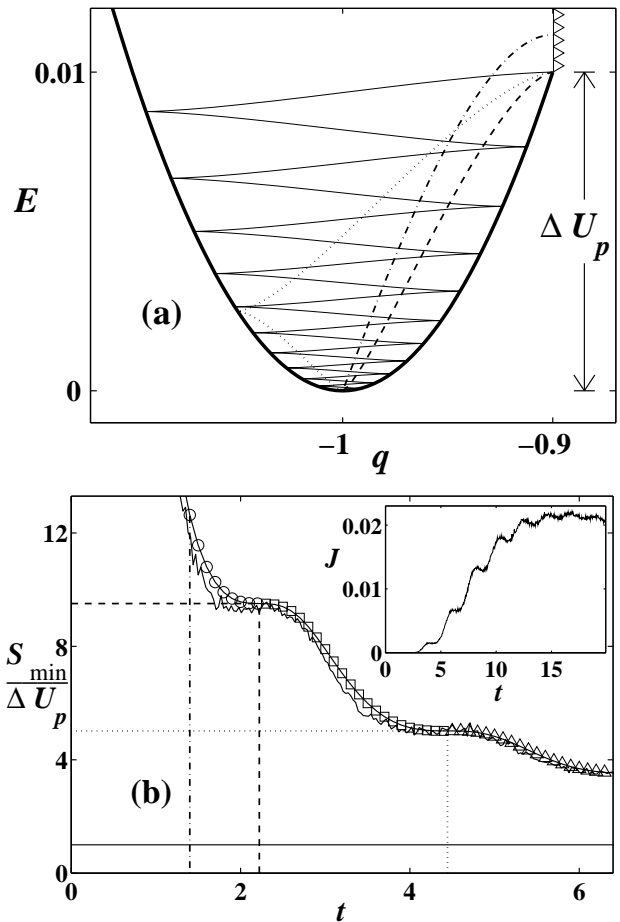


FIG. 2: The case of the bottom initial state. (a) The parabolic approximation $U_p(q) \equiv (q + 1)^2$ (thick solid line) of $U(q) - U(q_b)$ near the bottom, and examples of MPEPs (plotted in the energy-coordinate plane $E - q$ where $E \equiv \dot{q}^2/2 + U_p(q)$) at $\Gamma = 0.05$; the absorbing wall (at $q_{aw} = q_{aw}^{(1)} \equiv -0.9$) is indicated by triangles; (b) $S_{\min}(t)/\Delta U_p$ explicitly calculated in the parabolic approximation is shown by the solid line with markers: circles, squares and triangles indicate regions corresponding to respectively 0, 1 and 2 turning points in the MPEP; $S_{\min}(t)/\Delta U$ derived from simulations in $U(q)$ (3) is shown by the jagged line ($\Delta U \equiv U(q_{aw}) - U(q_b)$). Dashed and dotted lines indicate the theoretical 1st and 2nd inflection points with $dS_{\min}/dt = 0$, in (b), and the corresponding MPEPs, in (a). The thin solid line shows the large-time asymptote level ($= 1$), in (b), and the corresponding MPEP (which is the time-reversal of the noise-free trajectory from the state $(q = q_{aw}, \dot{q} = 0)$), in (a). The dash-dotted line shows in (a) the MPEP for some arbitrarily chosen time $t = 1.4$ (see (b)): it demonstrates that the exit velocity is typically non-zero. The inset shows $J(t)$ measured at $T = \Delta U$.

where $\omega_0 = \sqrt{2}$ and $q_b = -1$, in the case of $U(q)$ (3). Thus (15) reduces to a linear equation with constant coefficients that can be integrated explicitly. $S_{\min}(t)$ can be found explicitly too. Rather than presenting the cumbersome formulas, we discuss their most important consequence: if $\Gamma < 2\omega_0$, then $S_{\min}(t)$ has a step-

wise shape (Fig.2(b)) i.e. possesses inflection points with $dS_{\min}/dt = 0$ at

$$\begin{aligned} t = t_n &\equiv \frac{n\pi}{\omega_0 \sqrt{1 - (\Gamma/2\omega_0)^2}}, \\ S(t_n) &= \frac{\Delta U_p}{1 - \exp(-\Gamma t_n)}, \\ \Delta U_p &\equiv \omega_0^2 (q_{aw} - q_b)^2 / 2, \quad \Gamma < 2\omega_0, \quad n = 1, 2, 3, \dots \end{aligned} \quad (19)$$

The flux barely changes near t_n whereas it rises sharply beyond this range provided the corresponding n is not too large [37] (Fig.2(b)). In the underdamped case, the “length” of each step, $t_{n+1} - t_n$, is half a period of eigenoscillation and the “height” of the first steps is large: $S(t_n) - S(t_{n+1}) \approx \Delta U_p \omega_0 / (\pi \Gamma n(n+1)) \xrightarrow{\Gamma \rightarrow 0} \infty$. As Γ grows, the length of a step increases while the height decreases and, at $\Gamma = 2\omega_0$, the steps vanish.

The instants t_n mark intervals corresponding to different topologies of the MPEP: for $t \leq t_1$, $[q(\tau)]$ is monotonic while, for $t_n < t \leq t_{n+1}$ ($n = 1, 2, 3, \dots$), $[q(\tau)]$ possesses n turning points. As t changes, the MPEP varies *continuously* for any t , including $t = t_n$. The exit velocity is non-zero unless $t = t_n$ (Fig.2(a)).

Apart from a quantitative description of the case when the wall is close to the bottom of the well, the parabolic approximation provides qualitative estimates of the time and energy scales of the steps in the general case. However, some features of the steps $S_{\min}(t)$ and of the associated evolution of the MPEP change qualitatively as the absorbing wall moves towards the saddle.

Let us move the absorbing wall q_{aw} to a distinctly non-parabolic region of $U(q)$, but still not too close to the saddle ($< q_{aw}^{(c)}$). One can reduce the 4th-order differential equation (15) to a 2nd-order equation for q plus a 1st-order one for the auxiliary variable Γ' [32]:

$$\begin{aligned} \ddot{q} + \Gamma' \dot{q} + dU/dq &= 0 \\ [\dot{\Gamma}' + (\Gamma^2 - (\Gamma')^2)/2] \dot{q}^2 &= 2\Gamma \tilde{E}, \end{aligned} \quad (20)$$

where

$$\tilde{E} \equiv -\frac{\partial S}{\partial t} = -L + \left(\frac{\partial L}{\partial \dot{q}} - \frac{d}{dt} \left(\frac{\partial L}{\partial \ddot{q}} \right) \right) \dot{q} + \frac{\partial L}{\partial \ddot{q}} \ddot{q} \quad (21)$$

is conserved along the MPEP [32, 36], analogously to energy in mechanics [38]. Given that the initial state is at the bottom, it can be shown that $\tilde{E} \geq 0$ on the MPEP. Allowing for the fact that $\partial S/\partial \dot{q}(t) = 0$ on the MPEP,

$$\frac{dS_{\min}}{dt} = -\tilde{E}|_{\text{MPEP}} \leq 0. \quad (22)$$

The system (20), in addition to providing an algorithm [39] that is faster in some ranges of parameters than solving Eq. (15), has a remarkable feature: if $\tilde{E} = 0$,

the equation for Γ' can be integrated explicitly [32]. So, the 4th-order equation (15) reduces to a closed 2nd-order equation [40]. Allowing for $\dot{q}_i = 0$, the equation for the time-reversed trajectory $[\tilde{q}(\tau)] \equiv [q(t - \tau)]$ becomes

$$\begin{aligned} \frac{d^2 \tilde{q}}{d\tau^2} + \Gamma \frac{1 + Ae^{\Gamma\tau}}{1 - Ae^{\Gamma\tau}} \frac{d\tilde{q}}{d\tau} + \frac{dU(\tilde{q})}{d\tilde{q}} &= 0, \quad A = e^{-\Gamma t} \\ \tilde{q}(0) &= q_{aw}. \end{aligned} \quad (23)$$

For the sake of convenience, we have also presented in (23) the initial \tilde{q} which follows from the third of conditions (13). The derivative $d\tilde{q}(\tau = 0)/d\tau$ must be chosen such that the condition (16) is satisfied: comparing Eq.(23) at $\tau = 0$ with Eq.(16), we come to the important conclusion that

$$d\tilde{q}(\tau = 0)/d\tau = 0, \quad (24)$$

i.e. the MPEP has a zero exit velocity if $dS_{\min}/dt = 0$.

One can show (cf. [32]) that the number of possible finite values of t in eq.(23), such that $\tilde{q}(t) = q_b$, equals the number N of turning points in the noise-free ($t = \infty$) trajectory. Labelling such times t as $t_n \equiv t_n(q_{aw})$ ($n = 1, 2, \dots, N$), one may relate n to the number n_{tp} of turning points in the trajectory (23)-(24): $n = n_{tp} + 1$. t_n increases with n and, if $N = \infty$, the trajectory (23)-(24) for $t = t_n$ with $n \rightarrow \infty$ coincides with the noise-free trajectory. If

$$\Gamma < 2\omega_0, \quad (25)$$

then $N = \infty$ [32, 38] while, if $\Gamma \geq 2\omega_0$, then typically $N = 0$. In rare cases, there is a finite $N \neq 0$ at $\Gamma \geq 2\omega_0$ [32].

Thus, if $\Gamma < 2\omega_0$, then S_{\min} decreases with t monotonically, possessing an infinite number of inflection points t_n with $dS_{\min}(t_n)/dt_n = 0$ (Fig.3(a)). They divide the time axis into intervals where the MPEP has different numbers of turning points: as t increases, the transformation of the MPEP with $n - 1$ turning points, into one with n points, occurs *continuously* at $t = t_n$.

At $\tau = 0$, Eq.(23) coincides with the conventional relaxational equation with a *finite* friction parameter, $\Gamma \text{cth}(\Gamma t/2)$. Hence, the closer q_{aw} is to the saddle, the slower the motion near the wall. Thus, $t_n \rightarrow \infty$ if $q_{aw} \rightarrow q_s$. On the contrary, the time of motion along MPEPs which get to the wall with non-zero velocity (they relate to sections $S_{\min}(t)$ with non-zero dS_{\min}/dt) is less sensitive to the distance $q_s - q_{aw}$ and remains finite even if $q_{aw} = q_s$. Consequently, as q_{aw} grows, the onset of the *fold* at $t \approx t_1$ (according to numerical calculations) occurs at the critical value $q_{aw}^{(c)}$: dS_{\min}/dt is discontinuous at the fold (Fig.3(b)). At $q_{aw} > q_{aw}^{(c)}$, there are intervals of t during which the system (13),(15)-(17) possesses more than

one solution [41]. It is because, the closer q_{aw} is to q_s , the larger is the number of such intervals and the maximal possible number of coexisting solutions). This result provides a *multi-branch* structure for $S(t)$ satisfying (13),(15)-(17) (Fig.3(c)). In order to find the activation energy at a given t one should choose from the solutions of (13),(15)-(17) the minimal one. There are switches between different branches at certain critical times. These can be compared to switching processes, as other parameters vary, in certain escape problems [32, 34]; see also Sec. III.B below). The switches result in *jump-wise* changes of the MPEP while the activation energy still remains continuous (Fig.3(c)). At the same time, the switch results in a discontinuity dS_{\min}/dt : its values on different sides of the fold differ drastically, so that $S_{\min}(t)$ and $J(t)$ are still distinctly step-wise (Figs.3(c)).

We have tested some of the above predictions using computer simulations. $S_{\min}(t)$ is derived via optimal fitting of $J(t)$ obtained at different T . Figs. 2(b) and 3 show reasonable agreement between $S_{\min}(t)$ from the theory and from the simulations. The growth of the flux is clearly step-wise (see insets) in both cases.

2. Non-bottom initial state with a given coordinate and velocity

If the initial state with a given coordinate and velocity, $\{q_i, \dot{q}_i\}$, is shifted from the bottom of the well $\{q_b, 0\}$ then $S_{\min}(t)$ changes: cf. Fig.4. Typically, $S_{\min}(t)$ becomes non-monotonic: cf. Fig. 4(b) (only if $\dot{q}_i = 0$ it becomes step-wise i.e. monotonic: cf. Fig. 4(a)). Moreover, as is evident in Fig.4, even a tiny shift of the energy from the bottom results in quite a significant distortion of $S_{\min}(t)$: the shift of energy in Fig. 4(a) and Fig. 4(b) is equal to $\Delta U_p/100$ and $\Delta U_p/200$ respectively. Such strong sensitivity to the initial state can be explained by the singularity in the effective time-dependent damping parameter in equation (23), which describes the MPEP; so, the shift in the activation energy depends non-analytically on the shift of the energy of the initial state.

3. Thermalized initial state

A non-bottom initial state with a given coordinate and velocity might seem a rather artificial situation but, at the same time, there is always some non-zero initial temperature T_0 so that various non-bottom states are necessarily involved. The strong sensitivity of the flux $J_{q_i, \dot{q}_i}(t)$ to the shift of $\{q_i, \dot{q}_i\}$ from the bottom, appears to cast doubt on the generality of the stepwise growth J in real situations. However, a rigorous analysis (see below) shows that the flux at short time scales still grows in a stepwise manner for any temperature $T_0 < T$. Moreover, if $T_0/T \ll \Gamma/\omega_0$, then the step-wise structure for

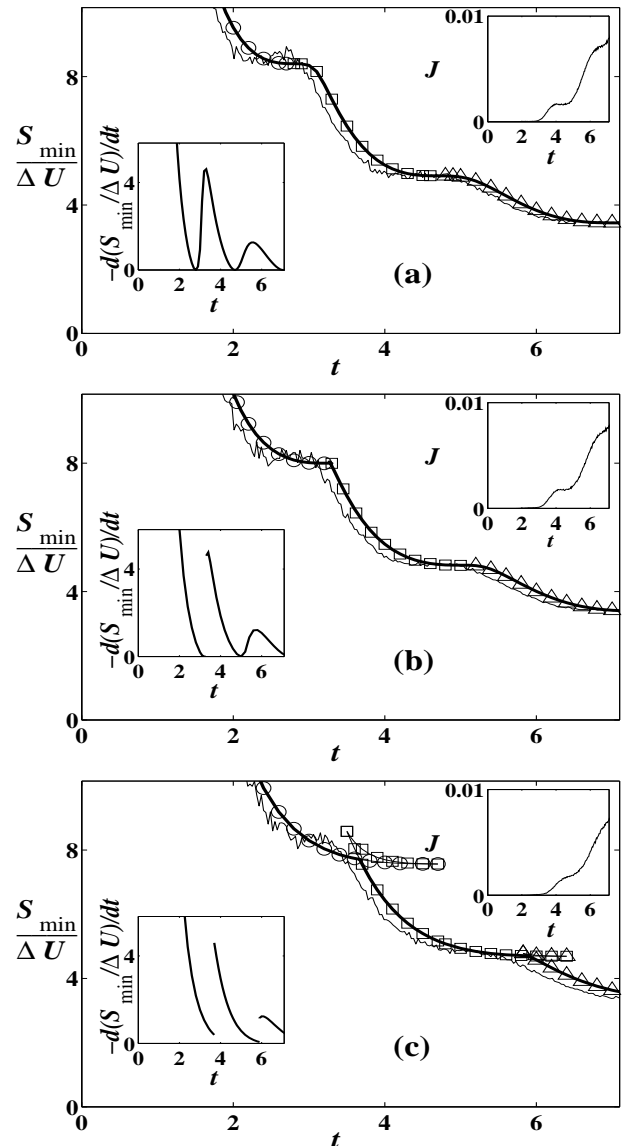


FIG. 3: The case of the bottom initial state. The evolution of $S_{\min}(t)$ normalized by $\Delta U \equiv U(q_{aw}) - U(q_b)$ (thick and jagged lines for the theory and simulations respectively) as q_{aw} increases: (a) $q_{aw} = q_{aw}^{(2)} \equiv 0$, (b) $q_{aw} = 0.371 \approx q_{aw}^{(c)}$, (c) $q_{aw} = q_{aw}^{(3)} \equiv 0.9$. $\Gamma = 0.05$. Branches of $S(t)$ corresponding to 0, 1 or 2 turning points in the escape path are shown by thin lines marked by circles, squares or triangles respectively: in (a) and (b), only one branch exists at each t while, in (c), a few branches coexist in some ranges of t (activation energy $S_{\min}(t)$ coincides with the lowest $S(t)$). Left and right insets show respectively $-d(S_{\min}(t)/\Delta U)/dt$ (theory) and $J(t)$ measured at $T = \Delta U$.

flux growth is similar to that obtained using the bottom as the initial state.

So, let the distribution of initial coordinates and velocities be quasi-stationary for some low temperature T_0 :

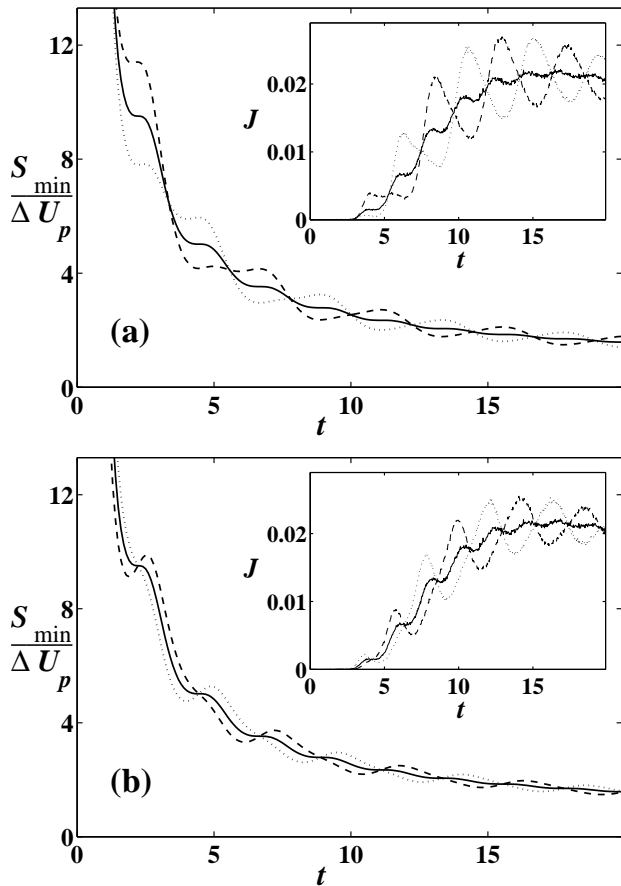


FIG. 4: Comparison between $S_{\min}(t)$ for the bottom initial state (solid line) and for two other initial states with given coordinate and velocity close to those in the bottom, with all other parameters the same as in Fig. 2: (a) $\dot{q}_0 = 0$ while $q_0 = q_b - 0.01$ (dotted line) or $q_0 = q_b + 0.01$ (dashed line); and (b) $q_0 = q_b$ while $\dot{q}_0 = -0.01$ (dotted line) or $\dot{q}_0 = 0.01$ (dashed line).

$$\begin{aligned}
 W_{in}(q_0, \dot{q}_0) &\approx W_{qs}(q_0, \dot{q}_0) \equiv \\
 &\equiv \begin{cases} \exp(-E_0/T_0)/Z & \text{for } E_0 < U(q_{aw}), \\ 0 & \text{for } E_0 > U(q_{aw}), \end{cases} \quad (26) \\
 E_0 &\equiv \dot{q}_0^2/2 + U(q_0), \\
 Z &= \int \int_{E_0 < U(q_{aw})} dq_0 d\dot{q}_0 \exp(-E_0/T_0).
 \end{aligned}$$

We assume that the probability for the system to leave the well before the relevant “initial” instant $t = 0$ is negligible.

If at the “initial” instant $t = 0$ the additional noise source is switched on, so that the effective temperature becomes $T > T_0$ [42], the evolution of the flux (6) with the initial distribution (26) becomes relevant. Given the activation-like structure of $J_{q_0, \dot{q}_0}(t)$ (eqs. (10)-(13)), the flux with the thermalized initial state can be presented in the form

$$J(t) \equiv J_{T_0}(t) = \tilde{P} e^{-\frac{\tilde{S}_{\min}(t)}{T}} \quad (27)$$

where \tilde{P} is some prefactor and \tilde{S}_{\min} is the generalized activation energy:

$$\tilde{S}_{\min} \equiv \tilde{S}_{\min}\left(\frac{T_0}{T}, t\right) = \min_{q_0, \dot{q}_0} \left\{ S_{\min}(q_0, \dot{q}_0, t) + \frac{T}{T_0} E_0 \right\}, \quad (28)$$

where $S_{\min}(q_0, \dot{q}_0, t)$ is given by (11)-(13) and E_0 is defined in (26).

There is no room here to provide details but it can be shown that, for any $T_0 < T$, the function $\tilde{S}_{\min}(\frac{T_0}{T}, t)$ is stepwise in t . Analogously to the case of the bottom initial state, \tilde{S}_{\min} possesses inflection points with $d\tilde{S}_{\min}/dt = 0$, provided the wall is not too close to the saddle, and the corresponding MPEPs are described by an equation similar to (23) but with the constant A related to t as

$$A = e^{-\Gamma t} \left(1 - \frac{T_0}{T}\right). \quad (29)$$

The relevant instants t are determined using the condition $\ddot{q}(t) = 0$, rather than the condition $\dot{q}(t) = q_b$ which is relevant to the bottom initial state.

It can be shown that $\tilde{S}_{\min}(\frac{T_0}{T}, t \sim \omega_0^{-1})$ is close to $S_{\min}(q_i = q_b, \dot{q}_i = 0, t \sim \omega_0^{-1})$ provided

$$\frac{T_0}{T} \ll \frac{\Gamma}{\omega_0}. \quad (30)$$

Otherwise $\tilde{S}_{\min}(t \sim \omega_0^{-1})$ is significantly lower and the steps are smeared (Fig. 5(b)).

The competition between the two small parameters, T_0/T and Γ/ω_0 , is readily interpreted physically. On one hand, the escape flux (on $t \sim \omega_0^{-1}$) from the bottom is $\propto \exp(-a\Delta U/(T\Gamma/\omega_0))$ where $a \equiv a(t) \sim 1$. On the other hand, if the system starts its motion from an energy E_0 close to the barrier level, the probability of escape for time $t \sim \omega_0^{-1}$ will be ~ 1 , but then the probability to have such starting energy is $\propto \exp(-\Delta U/T_0)$. It is the competition between these two exponentially weak processes which leads to the relation (30). Fig. 5(a) shows that, for $T_0/T = 0.01 \ll \Gamma/\omega_0 \approx 0.035$, the MPEP starts close to the bottom while, for $T_0/T = 0.2 \gg \Gamma/\omega_0$, the starting energy is $\sim \Delta U$.

B. Multi-well metastable potential

As an example of the multi-well case, we consider the potential (4), which describes the simplest SQUID [22]. We place an absorbing wall [27] at $q_{aw} = 4.5$ (Fig.6(a))

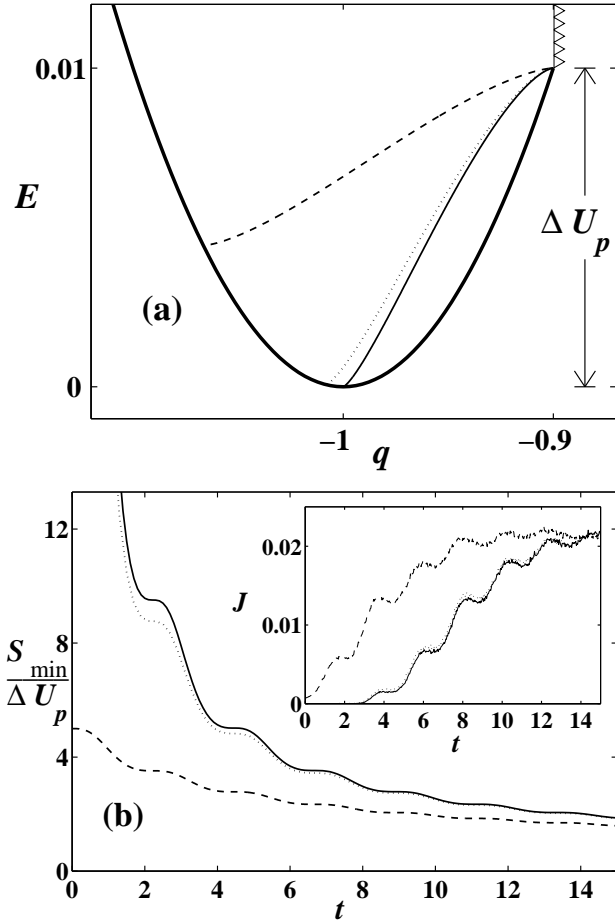


FIG. 5: The case of the thermalized initial state. (a) MPEPs for $t = 2.222$, for three characteristic values of T_0/T , with all other parameters the same as in Fig. 2: $T_0/T = 0$ (solid line), 0.01 (dotted line), 0.2 (dashed line); (b) $\tilde{S}_{\min}(t)$ for $T_0/T = 0$ (solid line), 0.01 (dotted line), 0.2 (dashed line).

while the initial state of the system (1),(4) may be any state within well-1; in simulations, we put it at the bottom of well-1, for the sake of simplicity. We emphasize also that the type of the boundary is not important either, e.g. our results are equally valid for the transition rates between non-adjacent wells in the stable potential with more than two wells [32].

Unlike the single-well case, where the formation time of quasi-equilibrium is of the order of $t_f^{(s)}$ (7), its formation in the multi-well case proceeds via two distinct stages: first, quasi-equilibrium is formed within the *initial well* which takes $t_f^{(1)} \sim t_f^{(s)}$: J evolves at this stage quite similarly [43] to the single-well case; secondly, quasi-equilibrium *between wells* becomes established which takes exponentially longer: $t_f^{(2)} \sim t_f^{(s)} \exp(\Delta U/T) \gg t_f^{(1)}$ where ΔU means a minimal internal barrier. During the latter stage, and during the subsequent quasi-stationary one, the flux $J(t)$ can be described via a solution of kinetic equations for the well populations, W_1 and W_2 , us-

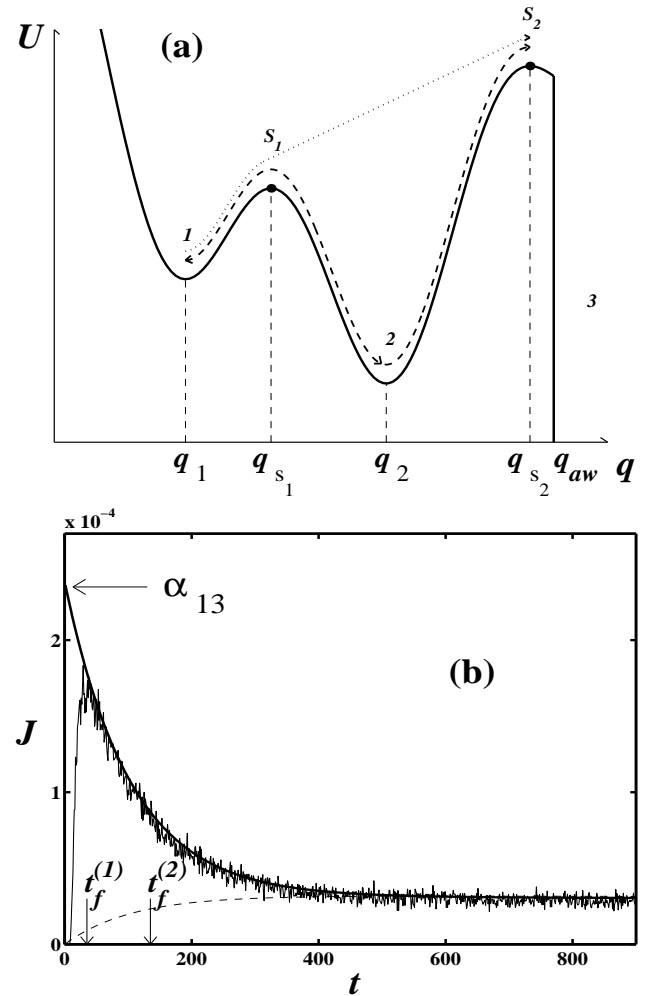


FIG. 6: (a) the potential (4) and a sketch of direct (dotted line) and indirect (dashed line) escape paths $1 \rightarrow s_2$; thin dashed lines indicate positions of the local minima (q_1, q_2) and maxima (q_{s_1}, q_{s_2}); (b) simulations of the dependence of the escape flux on time $J(t)$ (thin line) for the model (1),(4) at $\Gamma = 0.15$, $T = 0.4$. The thick full and dashed lines show the approximation of $J(t)$ by eq.(31) in which α_{12} , α_{21} , α_{qs} are calculated by the Kramers-Melnikov formula [3]. For the thick full line, $\alpha_{13,23} = \alpha_{qs}(1 + \{\Omega_1 \Omega_2^{-1} \exp[(U_1 - U_2)/T]\}^{\pm 1}) / (1 + \{m \exp[k S_{\min}(s_2 \rightarrow s_1)/T]\}^{\pm 1})$ where $\Omega_{1,2}$ are the frequencies of eigenoscillation in the bottom of wells 1,2 respectively, k is equal to 1,-1 for the ranges Γ providing $s_2 \xrightarrow{n_f} 2, 1$ respectively, $S_{\min}(s_2 \rightarrow s_1)$ is calculated from the theory [32] and m is the only adjustable parameter ($m \approx 1.1$ for these parameters); for the dashed line, $\alpha_{13} = 0$ and $\alpha_{23} = \alpha_{qs}(1 + \alpha_{21}/\alpha_{12})$.

ing the concept of constant inter-attractor [44] transition rates α_{ij} (cf. [45]):

$$J(t) \equiv W_1 \alpha_{13} + W_2 \alpha_{23} = \alpha_{13} e^{-\frac{t}{t_f^{(2)}}} + \alpha_{qs} \left(e^{-\frac{t}{t_{qs}}} - e^{-\frac{t}{t_f^{(2)}}} \right), \quad (31)$$

$$t_f^{(2)} \approx \alpha_{12}^{-1}, \quad t_{qs} \approx \alpha_{qs}^{-1} \approx \alpha_{12}/(\alpha_{12}\alpha_{23} + \alpha_{21}\alpha_{13}),$$

$$T \ll U_{s_1} - U_1, \quad t \gg t_f^{(1)}.$$

The physical meaning of the two terms in (31) is easily understood (cf. Fig. 6). The first one corresponds to *direct* escapes, i.e. those that do not go via the bottom of well-2, and it dominates until quasi-equilibrium becomes established. The second term, corresponding to indirect escapes, i.e. those that involve one or more intermediate transitions between wells 1 and 2 while the ultimate transition to 3 may occur from either well. It dominates during the ensuing quasi-stationary stage: it is the asymptotic part of this latter flux, $\alpha_{qs} \exp(-t/t_{qs})$, that is called the quasi-stationary flux.

Thus, in order to know the flux dynamics one needs to find the inter-well transition rates α_{ij} . The rates α_{12}, α_{21} and the quasi-stationary rate α_{qs} can be calculated from the Kramers-Melnikov formula [3]. Thus, only one of the four α_{ij} coefficients needs to be found independently. We choose α_{13} as the independent coefficient.

The theoretical problem of finding α_{13} is inherently difficult. Melnikov pointed out [3] that his method is valid in the multi-well case only if the barriers levels are equal or at least close to each other (cf. e.g. [3, 46]), a requirement that is often not satisfied. So, the method of *optimal fluctuation* (cf. the previous section) was suggested [32], seeking the escape rate in the form

$$\alpha_{13} = P e^{-\frac{S_{\min}}{T}}, \quad (32)$$

where the action S_{\min} does not depend on T and the dependence of the prefactor P on T is relatively weak.

One can show that S_{\min} is the minimum of a certain functional [32]

$$S_{\min} \equiv S_{\min}(1 \rightarrow s_2) = \min_{[q(t)], t_{tr}}(S), \quad (33)$$

$$S \equiv S_{t_{tr}}[q(t)] = \frac{1}{4\Gamma} \int_0^{t_{tr}} dt (\ddot{q} + \Gamma \dot{q} + dU/dq)^2,$$

$$q(0) = q_1, \quad \dot{q}(0) = 0, \quad q(t_{tr}) = q_{s_2}, \quad \dot{q}(t_{tr}) = 0,$$

where the trajectory $[q(t)]$ does not pass through attractor 2. It can easily be shown that the t_{tr} yielding S_{\min} is equal to ∞ . The $[q(t)]$ yielding S_{\min} is called [32] the *most probable direct transition path* (MPDTP). The main features of S_{\min} and the MPDTP are illustrated in Figs. 7 and 8 for the system (1),(4); see [32] for a rigorous general treatment [47].

Fig. 7 shows how the excess action

$$\Delta S \equiv \Delta S(1 \rightarrow s_2) = S_{\min}(1 \rightarrow s_2) - (U_{s_2} - U_1) \quad (34)$$

varies with Γ over the whole range of Γ , from very strong damping to the ultra-underdamped case. One can resolve three distinct regions.

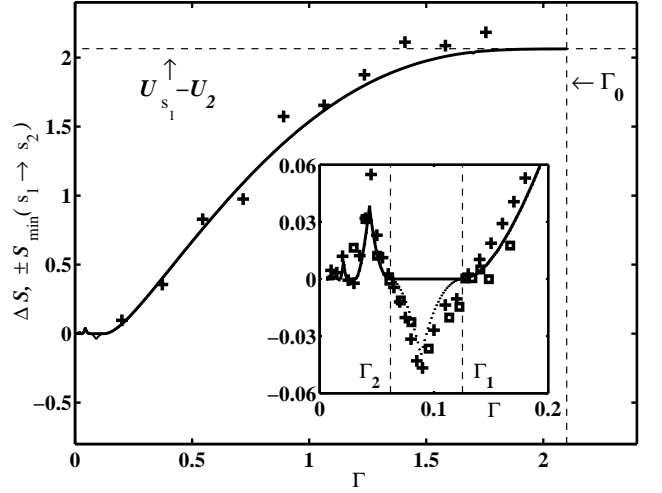


FIG. 7: Theoretical and experimental data on direct escapes/transitions in the metastable potential (4) (Fig.4(a)). The calculated excess of action over a difference of energies, $\Delta S(1 \rightarrow s_2)$ (34), is shown by the full line. It is related to the escape rate α_{13} . The calculated $\pm S_{\min}(s_2 \rightarrow s_1)$, related to R (37) by Eq.(38), is shown by the dotted line. It overlaps the full line in the half-plane of positive ordinates. The corresponding quantity (39) based on data obtained by electronic and computer simulations is shown by squares and crosses respectively. Values of $\Gamma_{n \geq 1}$ correspond to noise-free saddle-connections with $n-1$ turning points. At $\Gamma = \Gamma_0 = 2\Omega_2 \approx 2.1$, the turning points in the noise-free trajectories $s_2 \xrightarrow{n_f} 2$ and $s_1 \xrightarrow{n_f} 2$ disappear. The inset shows the low Γ range enlarged.

The overdamped region can be defined as $\Gamma \geq \Gamma_0 = 2\Omega_2$, where Ω_2 is the frequency of eigenoscillation in the bottom of well-2. Here, there is no MPDTP $1 \rightarrow s_2$ at all, so that $\alpha_{13} = 0$.

In the moderate-friction region, $[\Gamma_1, \Gamma_0]$, $\Delta S(\Gamma)$ is monotonic and undergoes its largest variation: from 0 to $U_{s_1} - U_2$. The MPDTP (see Fig. 8(a)) is the time-reversed trajectory $s_2 \xrightarrow{A=A_-} s_1 \xrightarrow{n_f} 1$ in which the latter is just the noise-free relaxation from s_1 to 1, whereas the former is the solution (cf. [35] and the previous section) of

$$\ddot{q}_d + \Gamma \frac{1 + Ae^{\Gamma t}}{1 - Ae^{\Gamma t}} \dot{q}_d + dU(q_d)/dq_d = 0, \quad (35)$$

$$q_d(0) = q_{s_2}, \quad \dot{q}_d(0) = 0,$$

$$q_d(t \rightarrow \infty) \rightarrow q_{s_1}, \quad \dot{q}_d(t \rightarrow \infty) \rightarrow 0.$$

Here $A = A_-$ is a negative constant providing for the minimal S among all values of A for which $[q_d(t)]$ reaches s_1 . Note that, in general, there may be an infinite set of A providing $[q_d(t)]$ connecting the saddles: the corresponding trajectories differ by their number of turning points.

The underdamped region, $\Gamma \leq \Gamma_1$, is divided by a number of characteristic values of the friction $\Gamma_{n \geq 1}$. Each of

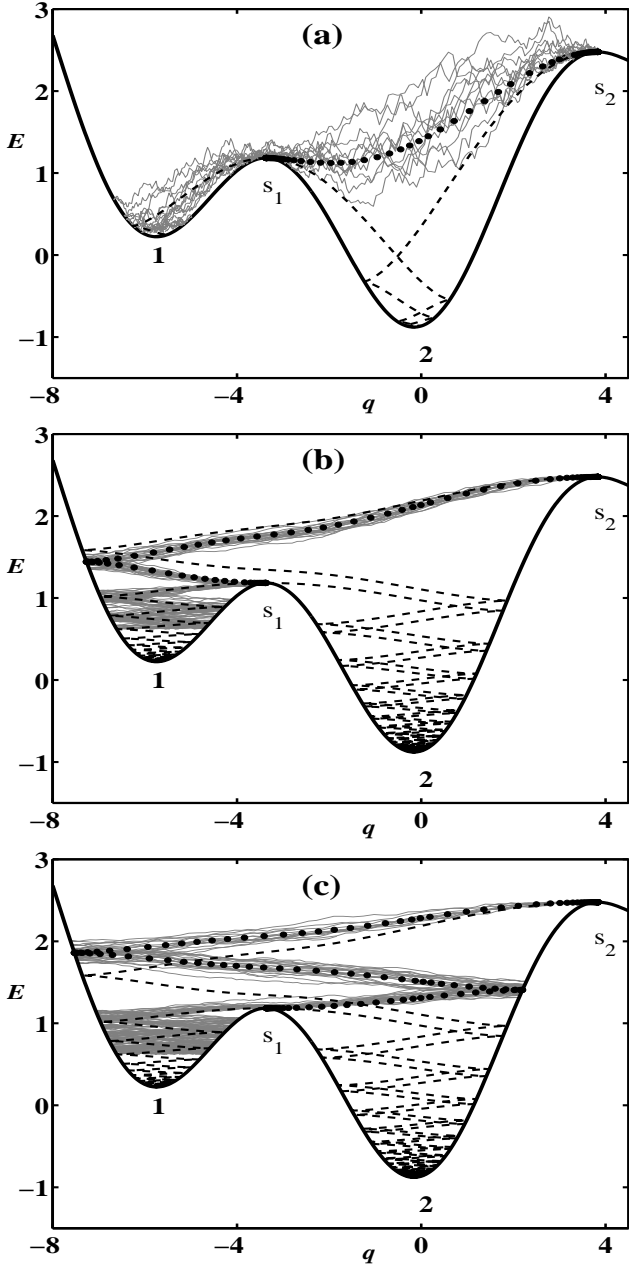


FIG. 8: Simulated direct transition paths $s_2 \rightarrow 1$ (thin full lines) in the energy-coordinate plane $E-q$ (where $E = \dot{q}^2/2 + U(q)$) corresponding to (1),(4) at different Γ : (a) 0.5, (b) 0.05, (c) 0.04 ($T = 0.05$ for (a) and $T = 0.005$ for (b), (c)). The noise-free trajectories $s_2 \xrightarrow{nf} 2$ and $s_1 \xrightarrow{nf} 1, 2$ are shown by dashed lines. The MPDTPs $s_2 \rightarrow s_1$ are shown by thick dotted lines.

these Γ_n provides for a *noise-free* saddle-connection $s_2 \xrightarrow{nf} s_1$, which possesses $n-1$ turning points. In this region, $\Delta S(\Gamma)$ undergoes oscillations corresponding to an alternation between two situations. In the first, $[\Gamma_{2m}, \Gamma_{2m-1}]$ ($m \geq 1$), a noise-free trajectory $s_2 \xrightarrow{nf} 1$ exists and the MPDTP is just its time-reversal, with $\Delta S = 0$. In the

second situation, $[\Gamma_{2m+1}, \Gamma_{2m}]$ ($m \geq 1$), the action varies nonmonotonically with Γ , and has cusps. This is due to a competition between the two paths which are the time-reversals respectively of $s_2 \xrightarrow{A_-} s_1 \xrightarrow{nf} 1$ and $s_2 \xrightarrow{A_+} s_1 \xrightarrow{nf} 1$, where $s_2 \xrightarrow{A_{\pm}} s_1$ are given by the solutions of (35) with $A_+ \equiv A_+(\Gamma) > 0$ and $A_- \equiv A_-(\Gamma) < 0$ respectively: see Fig.8(b) and Fig.8(c) respectively. As Γ varies, S along one path becomes equal to S along another, at a certain Γ , leading to switching between the paths and to the cusp in $\Delta S(\Gamma)$: there are corresponding discontinuities in the non-equilibrium potential [35] and fluctuational separatrix [48].

Thus, [32] predicts an exponentially strong dependence of the escape rate α_{13} on friction, including interesting features such as oscillations and cusps [49], for $t \gg t_f^{(1)}$. To establish whether these, and the properties of MPDTPs described above occur in reality, we have undertaken analogue electronic and computer simulations. A necessary condition is smallness of the temperature: $T \ll \Delta S, (U_{s_1} - U_1)$. However to obtain reasonable statistics at such a small temperature would require an unrealistically long time ($\propto \exp((U_{s_2} - U_1 + \Delta S)/T)$) [50]. We have overcome this difficulty by exploiting the property of detailed balance [51], which implies [32] that the MPDTP $s_2 \rightarrow 1$ is just the time-reversal of the MPDTP $1 \rightarrow s_2$, with the corresponding actions differing by $U_{s_2} - U_1$ i.e.

$$\Delta S(1 \rightarrow s_2) = S_{\min}(s_2 \rightarrow 1) = \begin{cases} 0 & \text{at } s_2 \xrightarrow{nf} 1, \\ S_{\min}(s_2 \rightarrow s_1) & \text{at } s_2 \xrightarrow{nf} 2, \end{cases} \quad (36)$$

so that information about the transition $s_2 \rightarrow 1$ is equivalent to that for $1 \rightarrow s_2$, but the experimental time required is of course much smaller in the former case ($\propto \exp(\Delta S/T)$) than in the latter.

Fig.8(a) demonstrates that, for $\Gamma \in [\Gamma_1, \Gamma_0]$, most of the direct paths $s_2 \rightarrow 1$ do indeed concentrate near $s_2 \xrightarrow{A_-} s_1 \xrightarrow{nf} 1$. Figures 8(b) and 8(c) demonstrate switching of the MPDTP from $s_2 \xrightarrow{A_+} s_1 \xrightarrow{nf} 1$ to $s_2 \xrightarrow{A_-} s_1 \xrightarrow{nf} 1$ as Γ decreases in the range $[\Gamma_3, \Gamma_2]$.

In order to study S_{\min} we use the following technique. The system is put at s_2 , and one then follows its stochastic dynamics (1),(4) until either the bottom of one of the wells is approached or the coordinate q_{aw} is reached. After that, the system is reset to s_2 and the operation is repeated. Once adequate statistics have been obtained, we calculate the ratio of transitions to wells 1 and 2 respectively:

$$R \equiv R(T) = \frac{N_{s_2 \rightarrow 1}}{N_{s_2 \rightarrow 2}}. \quad (37)$$

It is easy to see that $R \propto \exp(\pm S_{\min}(s_2 \rightarrow s_1)/T)$ (where $+, -$ correspond to ranges of Γ providing $s_2 \xrightarrow{nf} 1, 2$ respectively). So, $S_{\min}(s_2 \rightarrow s_1)$ is related to R (37) as

$$\pm S_{\min}(s_2 \rightarrow s_1) = \lim_{T \rightarrow 0} [T \ln(R(T))], \quad (38)$$

where $+$, $-$ correspond to $s_2 \xrightarrow{n_f} 1, 2$ respectively.

In practice, however, there is always a lower limit for T in simulations, T_l , because the overall simulation time must not become unrealistically long. That is why the use of (38) may, in practice, introduce significant inaccuracy. To reduce the influence of the pre-exponential factor we measure R both at T_l and at a slightly higher temperature, $T_l + \Delta T$ ($T_l \gg \Delta T \gtrsim T_l^2/S_{\min}(s_2 \rightarrow s_1)$), so that:

$$\pm S_{\min}(s_2 \rightarrow s_1) \approx \frac{T_l^2}{\Delta T} \ln\left(\frac{R(T_l + \Delta T)}{R(T_l)}\right). \quad (39)$$

The quantities on the left and right of Eq. (39) are shown in Fig.7 respectively by the dotted line (theory) and by squares and crosses (electronic and computer simulations respectively). The agreement is satisfactory, given that $5 \lesssim S_{\min}/T_l \lesssim 7$.

Note that the magnitude of the largest oscillation in action may significantly exceed $U_{s_2} - U_1$. This occurs if the initial well-1 is adjacent to an external saddle s_2 while its depth is much less than that of the other well.

Finally, we comment on the experimental consequence of the cutoff of the MPDTP, namely the drastic change of the time evolution of J for $t_f^{(1)} \lesssim t \ll t_f^{(2)}$: at $\Gamma < \Gamma_0$, one may in principle make T small enough that the sharp growth of $J(t)$ at $t \gtrsim t_f^{(1)}$ turns into a nearly constant value at $t_f^{(1)} \ll t \ll t_f^{(1)}\alpha_{13}/(\alpha_{12}\alpha_{23})$ while, at $\Gamma > \Gamma_0$, $J(t) \approx \alpha_{12}\alpha_{23}t$ over the whole relevant time-scale: cf. the thin full and dashed lines in Fig.6(b).

IV. ROADMAP FOR THE SUBJECT

In this section, we briefly discuss potentially interesting directions of a development of the subject in future both science-wise and for applications, in the subsections A and B respectively.

A. Scientific directions

It is convenient to formulate open problems for the ranges $t \ll t_f^{(s)}$ and $t_f^{(1)} \ll t \lesssim t_f^{(2)}$ separately.

1. *Range of times being much less than time of the formation of quasi-equilibrium within a single/initial area of phase space*

It would be interesting to study the following issues.

1. Details of the case considered above, including in particular an accurate study of: (i) oscillations of the exit velocity and dS_{\min}/dt as the exit time goes, as well as (ii) the transition from a smooth $S_{\min}(t)$, with inflection points only, to an $S_{\min}(t)$ possessing folds.
2. Additional features characteristic of other types of boundary or other types of transitions, in particular inter-well transitions in the symmetric double-well potential - the case particularly relevant in the context of some promising application (see Sec. IV.B.1 below).
3. A careful consideration of the case with two absorbing walls while the initial coordinate is close to one of the walls and the initial velocity is directed towards the opposite wall, a case that is relevant e.g. to ionic channels [52–54]. The preliminary analysis indicates oscillations of the flux in time.
4. Generalization for non-potential systems and/or non-white noise for which, unlike potential systems subject to white noise where switching between different MPEPs gives rise only to folds in $S_{\min}(t)$, we anticipate the possibility of jumps in $S_{\min}(t)$. Of a particular interest, the cases of various low-frequency noises [55] and quasi-resonant noise [8] are since they relate to many real systems.

5. Pre-exponential factor.

6. Multi-dimensional problems.

2. *For the multi-equilibria case only: range of times in between the time-scale of the formation of quasi-equilibrium within the single well/area and that within all wells or, more generally, areas of attraction of all attractors*

1. The case with more than two barriers.

2. Pre-exponential factor.

3. Multi-dimensional problems.

B. Applications

There may be various applications of the results described above. We restrict ourselves to a description of just two of them, which seem to us most promising.

1. *Measurements of noise intensity in a huge range*

Thermometers or, more generally, meters of noise intensity, which we call further as *noisemeters* typically can measure temperature or noise intensity respectively in a

quite limited range only. In other words, the lower and upper limits of measurements are of the same order of magnitude or, at best, they differ by 1-2 orders of magnitude only. For example, a common room thermometer can measure temperature just in the range 280-320 K.

Generally speaking, an estimate of temperature or noise intensity in case of a non-thermal noise (for the sake of brevity, we shall use one and the same notation T for both cases) can also be based on a measurement of a quasi-stationary noise-induced escape flux. However, to the best of our knowledge, for real routine estimates of T (i.e. for everyday or engineering purposes rather than for just scientific ones) it has not been used. Perhaps, the reason of this is the following: on the one hand, such a measurement is rather time-consuming and, on the other hand, the range of T which can be thus measured is not very large. As for the lower limit, it is about $T_{qs}^{(l)} \approx \Delta U/12$, where $\Delta U \equiv U(q_{aw}) - U(q_b)$ is the value of the “barrier” for a given value q_{aw} (the lowest possible ΔU is limited with the lowest value of $q_{aw} - q_b$ which is possible to measure sufficiently accurately) while the denominator 12 is explained by that, for larger values of the denominator, the escape probability is so low that it is impossible to measure the escape flux for a realistic time [56]. The main restriction for the estimate of T by means of the measurement of the *quasi-stationary* escape flux relates to the upper limit of T which can thus be measured: it is inherently limited from above with the value $T_{qs}^{(up)} \approx \Delta U_{max}/3$, where $\Delta U_{max} \equiv U(q_s) - U(q_b)$ is the maximal possible value of the potential barrier (cf. Fig. 1). For larger values of T , the exponential (activation-like) factor in the dependence of the escape rate α_{qs} (2) on T is not sufficiently sharp and the Kramers-Melnikov formula for α_{qs} [1–3] is not valid anymore. The restriction for the upper limit $T_{qs}^{(up)}$ is especially important in case of a non-thermal noise as such a noise may have a very large intensity and, moreover, its variation may be very large (constituting many orders of magnitude).

Our results for the noise-induced escape at time-scales much less than the scale of the formation of the quasi-equilibrium in a single well $t_f^{(s)}$ (7) (i.e. those described in Sec. III.A) in case of low friction, which is relevant first of all to nano/micro-mechanical resonators, promise to provide a possibility to measure noise intensity in the range varying by many orders of magnitude while using *one and the same* device. Application-wise it may provide a great financial benefit.

There is no room here to provide details [57]. Rather we just give the main ideas and mention a few difficulties which may be encountered. We see two distinctly different options for an implementation of our ideas.

1. *The setup with an “absorbing” wall.* As compared with the second option described below, the present setup allows us to immediately utilize the results presented in Sec. III.A (in particular, the explicit

results for the parabolic approximation of the potential) and, besides, it might be favourable in terms of the duration of the required measurements and of the computation time required for the calculation of T from the measurements. At the same time, the setup might give rise to a serious technical problem: each time when the system reaches the “wall” (being, in fact, just a given coordinate rather than a real wall), it should be somehow returned into the initial state (i.e. in the bottom of the well), and it is desirable for this transition to occur quickly, which may not be easily feasible. Generally speaking, such a return might be fulfilled by means of an interruption of an action of noise on the system (e.g., if noise acts due to an electric connection, then the corresponding connection may be switched off). Then, the time-scale for a single return is Γ^{-1} . If there is a possibility to strongly increase the dissipation, then the time-scale would further gratefully decrease. Another possibility is to introduce some additional action on the system which would transfer the system into the vicinity of the bottom of the well. We do realize that the problem of a fast return into the bottom of the well after reaching the coordinate q_{aw} may not be trivial in reality, but meanwhile we assume that it can be resolved somehow.

Let us discuss the key points of the algorithm of the measurements. Firstly, we should roughly estimate the quasi-stationary escape rate α_{qs} . To this end, it would be sufficient to observe just a few (up to 10) escapes and average them, thus obtaining the rough estimate for α_{qs} .

If the relation $\alpha_{qs} \ll \Gamma$ holds true, then we may conclude that $T \ll \Delta U$ and therefore the Kramers formula for α_{qs} [1–4] may be readily used, so that we just need to gain more statistics in order to measure α_{qs} more accurately and then to calculate T from it by means of the Kramers formula.

Of the main interest in the present context is the complementary case: $\alpha_{qs} \gtrsim \Gamma$. It follows from this relation that $T \gtrsim \Delta U$. In this case, we should measure the flux at relatively small time-scales namely at $t \ll t_{esc} \equiv \alpha_{qs}^{-1}$. In order to obey this inequality while avoiding too poor statistics we should choose a compromise, namely to explore the time $t \approx t^{(N)} \equiv t_{esc}/N$ where N is a moderately large number (about 5 – 6). Then we need to compare $t^{(N)}$ with the step width, i.e. with π/ω_0 . If $t^{(N)} \gg \pi/\omega_0$, then the step structure is smeared at the time-scale $t^{(N)}$. It is convenient in this case to measure the escape flux at $t = t^{(N)}$ and $t = t^{(N+1)}$ and to compare with each other while T can be shown to obey the following formula:

$$T = \frac{\Delta U}{\Gamma t_{esc} \ln \left(\frac{J(t^{(N)})}{J(t^{(N+1)})} \right)}, \quad \frac{\pi}{\omega_0} \ll t^{(N)} \lesssim \frac{1}{\Gamma}, \quad (40)$$

$$t^{(K)} \equiv \frac{t_{esc}}{K}, \quad t_{esc} \equiv \alpha_{qs}^{-1}, \quad N \approx 6.$$

If $t^{(N)}$ is of the same order as π/ω_0 , then it may be preferable to measure the flux at the centers of the first and second steps rather than at $t^{(N)}$ and $t^{(N+1)}$: the results are much less sensitive to an inaccuracy of a measurement of time. Using formulas in Eq. (19), we obtain:

$$T = \Delta U \frac{\omega_0/(2\pi\Gamma)}{\ln(J(t_2)/J(t_1))}, \quad \frac{t_{esc}}{6} \sim \frac{\pi}{\omega_0}, \quad (41)$$

where t_n is defined in (19).

Finally, if $t^{(N)} \ll \pi/\omega_0$, then one should use the function $S_{min}(t)$ calculated for $t = t^{(N)}$ and $t = t^{(N+1)}$ by methods described in Sec. III.A. Then T can be calculated by means of the formula which is formally valid in a general form for any time-scale and for any position of q_{aw} :

$$T = \frac{S_{min}(t^{(N+1)}) - S_{min}(t^{(N)})}{\ln \left(\frac{J(t^{(N)})}{J(t^{(N+1)})} \right)}, \quad (42)$$

where $t^{(K)}$ and N are defined in Eq. (40) and we do not restrict the range of its validity to $t^{(N)} \ll \pi/\omega_0$ since Eq. (42) is valid in the much broader range: $t^{(N)} \lesssim \Gamma^{-1}$ (Eq. (40) represents a partial case of (42) provided q_{aw} lies sufficiently close to the bottom of the well, so that the parabolic approximation of $U(q)$ works well). Of course, various inaccuracies of experimental measurements and theoretical approximations put a limit for the lowest limit of the range of $t^{(N)}$ where Eq. (42) is valid and this determines the upper limit for values of T which we can measure by means of such a method. The limitations will be discussed elsewhere.

Even if to skip the range of very small times and to restrict ourselves to the range $t_{esc}/6 \gtrsim \pi/\omega_0$, we can see from Eqs. (40) and (41) that our approach allows one to measure T within the range characterized with the ratio of an upper and lower limits of the order of the quality factor $Q \equiv \omega_0/\Gamma$. A few more orders of magnitude may be added for the account of a decrease of an effective ΔU (by means of shifting q_{aw} closer to the bottom of the well). Quality factors of modern nano/micro-mechanical resonators can rather easily reach values $10^6 - 10^7$ [8, 23, 58] and therefore our method provides a possibility to measure T with one and the same device within a huge range of the order of $10^8 - 10^{10}$.

2. *The setup with transitions between bottoms of wells of a symmetric double-well potential.* If we use a device characterized with a symmetric double-well potential (for example, it may be a buckled doubly-clamped beam [59] or a nanoparticle levitating in a bistable one-dimensional optical trap [24]) and consider transitions between close vicinities of bottoms of the potential wells, then the transitions in both directions are equivalent in the context of the transition probability and transition flux. Therefore there is no need to artificially return the system into the initial state. As compared with the setup with the absorbing wall, this is a big advantage. One of disadvantages consists in that we cannot vary the magnitude of an effective barrier ΔU . Besides, it is necessary to generalize the theory for this case, and the results certainly will not be expressed explicitly. On the other hand, the latter disadvantage (a necessity to use a complicated numerical procedure for a calculation $S_{min}(t)$) is not crucial: for a given potential $U(q)$, one will be able to calculate $S_{min}(t)$ once and forever, so that it will be used just as a known numerical function for any new measurement.

We conclude this sub-section with the formulation of its main idea in an alternative form. We suggest to replace a straightforward measurement of temperature T (or its equivalent in case of noise of a non-thermal origin) for a measurement of the escape/transition flux in an appropriate time range. The method allows to measure T in a huge range using the following idea. When T is of the order of or larger than an effective potential "barrier" in our system, then, knowing the theoretical dependence of the activation barrier on the time of a given noise-induced escape/transition, we can measure the relevant escape/transition time at which the activation barrier corresponds to the relevant flux. If a clock used in the time measurements exploits a periodic process with a very small period, then the clock can measure time in a huge range, being much larger than ranges in which a measurement of temperature by means of straightforward methods can be done. In a sense, *we suggest to reduce a measurement of temperature to a measurement of time while the latter can be measured in a much larger range than temperature can be conventionally measured.*

2. Accurate measurement of a damping parameter

A linear damping parameter Γ of an underdamped oscillator is typically measured as a half-width of a resonance curve in case when noise is absent (or negligible) while the driving amplitude is sufficiently small for a nonlinearity to play a negligible role for constrained vibrations (see e.g. [8]). Such measurements are not very

accurate however. Results reviewed in this paper might provide a method of a much more accurate measurement of a linear damping. We briefly describe it below.

We assume that we know temperature T in the system and $U(q)$ in some vicinity to the bottom of the well with a high accuracy. Then we should *roughly* measure/estimate Γ (which can be done with a few methods). As described in the previous item IV.B.1, we can readily define the value of q_{aw} and choose time $t = t^{(N)}$ so that the corresponding action $S_{min}(t^{(N)})$ exceeds T with the optimal factor $N = 5 - 6$. Given that action is inversely proportional to Γ , the flux $J(t^{(N)})$ depends on Γ in the activation-like manner i.e. very sharply. At the same time, the statistics of escapes is not too poor (due to that $N = 5 - 6$ is just *moderately* large), so that the flux can be measured with a high accuracy while the accuracy of the estimate of Γ from the flux measurements is even larger with the factor of the order of N .

CONCLUSIONS

Our paper reviews results on noise-induced escapes and transitions at time-scales preceding the formation of equilibrium/quasi-equilibrium for the case of white noise and linear damping with a small or moderate value of the damping parameter Γ , and discuss interesting open problems as well as a couple of promising applications.

The escapes/transitions at small time-scales occur quite differently from those at time-scales exceeding the time-scale of the equilibrium/quasi-equilibrium formation $t_{qe} \sim \Gamma^{-1}$, and the corresponding probability flux is exponentially smaller. The strongest difference concerns the case of small damping ($\Gamma \ll \omega_0$, where ω_0 is a frequency of weak eigenoscillations of the system), and the smaller the escape/transition time t is, the larger the difference is. Roughly speaking, the activation energy S_{min} for the escape/transition at time t is of the order of $\Delta U/(\Gamma t)$, where ΔU is a relevant potential barrier or a difference of relevant energies. Thus, for the relevant range $t \ll \Gamma^{-1}$, the activation energy $S_{min}(t \ll \Gamma^{-1})$ greatly exceeds the conventional activation energy ΔU for the quasi-stationary flux. As t decreases, a topology of the most probable escape path (MPEP) changes: a number of turning points decreases at such values of t . Sometimes, this results in a continuous change of the MPEP and, sometimes, in a jump-wise change. The most interesting feature of the function $S_{min}(t)$ is its step-wise form, which is due to the aforementioned change of the MPEP topology. The time-scale of the step is $\sim \pi/\omega_0$, and steps are most distinct at times t of the order of the period of the eigenoscillation.

For potentials with more than one barrier, the direct escape flux over both barriers is characterized with the activation energy S_{dir} which, as function of Γ , undergoes oscillations in the range small values of Γ and a large in-

crease in the range of moderate values (typically limited from above by the value $2\omega_0$). These variations are related to variations of the MPEP, including in particular the variation of its topology responsible for the oscillations in $S_{dir}(\Gamma)$.

We also briefly discuss various open related problems which seem to us interesting and, in somewhat larger detail a couple of potential applications, namely: (i) a measurement of temperature or of noise intensity of a non-thermal noise in a very broad range, (ii) a rather accurate measurement of the damping parameter.

ACKNOWLEDGEMENTS

We acknowledge discussions with Mark Dykman, Yuri Rubo and Yuri Semenov.

* Electronic address: stanislav.soskin@gmail.com

† Electronic address: linnik1971@hotmail.com

- [1] V.I. Mel'nikov, "Activated tunneling decay of metastable states", Zh. Exp. Teor. Fiz. **87**, 663-673 (1984); Sov. Phys. JETP, **60**, 380-385 (1984).
- [2] V.I. Mel'nikov, S.V. Meshkov, "Theory of activated rate processes: Exact solution of the Kramers problem", J. Chem. Phys. **85**, 1018-1027 (1986).
- [3] V.I. Mel'nikov, "The Kramers problem: fifty years of development", Phys. Rep. **209**, 1-71 (1991).
- [4] H.A. Kramers, "Brownian Motion in a Field of Force and the Diffusion Model of Chemical Reactions", Physica **7**, 284-304 (1940).
- [5] S.M. Soskin, "Fluctuation spectrum peaks for systems where the oscillation frequency dependence on energy has an extremum", Physica A **155**, 401-429 (1989).
- [6] S.M. Soskin, R. Mannella and P.V.E. McClintock, "Zero-Dispersion Phenomena in oscillatory systems", Phys. Rep. **373**, 247-409 (2003).
- [7] S.M. Soskin, R. Mannella, O.M. Yevtushenko, I.A. Khovanov and P.V.E. McClintock, "A New Approach To The Treatment Of Separatrix Chaos", Fluct. Noise Lett. **11**, 1240002-1-1240002-12 (2012).
- [8] L. Huang, S.M. Soskin, I.A. Khovanov, R. Mannella, K. Ninos and H.B. Chan, "Frequency stabilization and noise-induced spectral narrowing in resonators with zero dispersion", Nature Communications **10**, 3930-1-3930-10 (2019).
- [9] R.P. Feynman, *Statistical Mechanics*, Benjamin, Reading, Massachusetts, 1972.
- [10] R.P. Feynman and A.R. Hibbs, *Quantum Mechanics and Path Integrals* (McGraw-Hill, New York, 1965); Russian translation: R. Feinman, A. Hibbs, *Kvantovaya Mehanika i integraly po traektoriyam*, Mir, Moskva, 1968.
- [11] S.M. Soskin, V.I. Sheka, T.L. Linnik, M. Arrayas, I.Kh. Kaufman, D.G. Luchinsky, P.V.E. McClintock and R. Mannella, "Kramers problem: beyond quasi-stationarity", in *Stochastic and chaotic dynamics in Lakes*, ed. D.S. Broomhead, E.A. Luchinskaya, P.V.E.

- McClintock and T. Mullin (American Institute of Physics, Melville, NY, USA, 2000), pp. 60-68.
- [12] S.M. Soskin, V.I. Sheka, T.L. Linnik, and R. Mannella, “Short time-scales in the Kramers problem: a step-wise growth of escape flux”, *Phys. Rev. Lett.* **86**, 1665-1669 (2001).
- [13] S.M. Soskin, V.I. Sheka, T.L. Linnik, and R. Mannella, “Erratum for “Short time-scales in the Kramers problem: a step-wise growth of escape flux””, *Phys. Rev. Lett.* **87**, 059901(E) (2001).
- [14] S.M. Soskin, V.I. Sheka, T.L. Linnik, and R. Mannella, “Characteristic types of evolution of noise-induced escape flux at short time scales”, *Fluct. Noise Lett.* **1**, L87-L95 (2001).
- [15] S.M. Soskin, V.I. Sheka, T.L. Linnik, M. Arrayas, I.Kh. Kaufman, D.G. Luchinsky, P.V.E. McClintock, and R. Mannella, “Noise-induced escape on time scales preceding quasistationarity: New developments in the Kramers problem”, *Chaos* **11**, 595-604 (2001).
- [16] S.M. Soskin, V.I. Sheka, T.L. Linnik, and R. Mannella, “Escapes and transitions in overdamped systems on short times: general solution”, in *Unsolved Problems of Noise and Fluctuations*, eds. L. Reggiani, C. Penneta, V. Akimov, E. Alfinito, M. Rosini (American Institute of Physics, Melville, NY, USA, 2005), AIP Conference Proceedings Volume 800, pp. 262-269.
- [17] S.M. Soskin, V.I. Sheka, T.L. Linnik, and R. Mannella, “Short-time dynamics of noise-induced escapes and transitions in overdamped systems”, *Semiconductor Physics, Quantum Electronics & Optoelectronics* **25**, 262-274 (2022).
- [18] S.M. Soskin, “Most probable transition path in an overdamped system for a finite transition time”, *Phys. Lett. A* **353**, 281-290 (2006).
- [19] E.I. Rashba and V.I. Sheka, “Symmetry of Energy Bands in Crystals of Wurtzite Type II. Symmetry of Bands with Spin-Orbit Interaction Included”, *Fiz. Tverd. Tela: Collected Papers* **2**, 62–76 (1959); English translation is published as the supplementary material to the article by Bihlmayer et al., *New. J. Phys.* **17**, 050202 (2015) being available at stacks.iop.org/NJP/17/050202/mmedia.
- [20] V.I. Sheka and T.L. Linnik, *Metod Invariantov v Teorii Poluprovodnikov* (Vinnichenko, Kiev, 2017), in Russian.
- [21] G.L. Bir and G.E. Pikus, *Simmetriya i deformacionnye efekty v poluprovodnikah* (Nauka, Moscow, 1972), in Russian. English translation: *Symmetry and Strain-Induced Effects in Semiconductors* (Wiley, New York, 1974).
- [22] K.K. Likharev, *Dynamics of Josephson Junctions and Circuits* (Gordon and Breach, Philadelphia, 1986).
- [23] A. Bachtold, J. Moser, M.I. Dykman, “Mesoscopic physics of nanomechanical systems”, arXiv:2202.01819 [cond-mat.mes-hall].
- [24] J. Flajsmanova, M. Siler, P. Jedlicka, F. Hrubý, O. Brzobohatý, R. Filip and P. Zemánek, “Using the transient trajectories of an optically levitated nanoparticle to characterize a stochastic Duffing oscillator”, *Sci. Rep.* **10**, 14436 (2020).
- [25] V.A. Shneidman, “Transient solution of the Kramers problem in the weak noise limit”, *Phys. Rev. E* **56**, 5257 (1997).
- [26] E.W.G. Diau, J.L. Herek, Z.H. Kim, and A.H. Zewail, “Femtosecond Activation of Reactions and the Concept of Nonergodic Molecules” *Science* **279**, 847 (1998).
- [27] The absorbing wall is equivalent to the barrier falling down to $-\infty$, which is illustrated by Fig. 6(a).
- [28] The choice of t_l is quite arbitrary: it should exceed the relevant time-scale and is introduced purely to reduce the overall time of experiment.
- [29] M.I. Dykman, P.V. E. McClintock, V.N. Smelyanski, N.D. Stein and N.G. Stocks, “Optimal paths and the prehistory problem for large fluctuations in noise-driven systems”, *Phys. Rev. Lett.* **68**, 2718 (1992).
- [30] If the wall is close to the bottom, the estimate (7) can be obtained by consideration of the parabolic potential: the Fokker-Plank equation is then solved explicitly [31]. It follows directly that, if the initial state corresponds to the bottom of the well i.e. $W(q, \dot{q}, t = 0) = \delta(q - q_b)\delta(\dot{q})$, then $W(q = \sqrt{2\Delta U}/\omega_0, \dot{q} = 0, t)$ evolves close to the equilibrium value for the time described by Eq.(7). In another characteristic case, when the wall is close to the saddle (cf. $q_{aw}^{(3)}$ in Fig.1), the estimate (7) is also typically valid: it agrees with the explicit results [25] for the underdamped and overdamped limits provided that the curvatures at the saddle and at the bottom are of the same order, which is typically the case: cf. $U(q)$ (1).
- [31] M.C. Wang, G.E. Uhlenbeck, “On the Theory of the Brownian Motion II”, *Rev. Mod. Phys.* **17**, 323 (1945).
- [32] S.M. Soskin, “Large fluctuations in multi-attractor systems and the generalized Kramers problem”, *J. Stat. Phys.* **97**, 609 (1999).
- [33] Note that the minimization over the exit velocity (or, more generally, over states on a relevant boundary) was not used in applications of the method of optimal fluctuation to *quasi-stationary* escape rates [32, 34] or related quantities [35] since the exit occurred necessarily through the saddle.
- [34] R.S. Maier, D.L. Stein, “A scaling theory of bifurcations in the symmetric weak-noise escape problem” *J. Stat. Phys.* **83**, 291 (1996).
- [35] R. Graham and T. Tel, “Nonequilibrium potential for coexisting attractors” *Phys. Rev. A* **33**, 1322 (1986).
- [36] L.E. Elsgolc *Calculus of Variations*, (Pergamon Press, London, 1961).
- [37] If $n \rightarrow \infty$, so that $t_n \rightarrow \infty$, then $S(t_n)$ reduces to ΔU_p while the MPEP reduces to the time-reversal of the noise-free relaxation trajectory from the state $\{q = q_{aw}, \dot{q} = 0\}$, thus recovering the conventional Arrhenius activation energy for the quasi-stationary flux (Refs. 1-4) and the corresponding MPEP (Refs. 34 and 31), respectively. The reduction of the asymptotic (at $t \rightarrow \infty$) activation energy and MPEP to their conventional forms is valid for an arbitrary $U(q)$.
- [38] L.D. Landau and E.M. Lifshitz *Mechanics*, (Pergamon, London, 1976).
- [39] To avoid the singularities encountered by Γ' at the turning points, one may use the variable $G \equiv \Gamma' \dot{q}$ instead.
- [40] A similar equation was obtained in Ref. 34 but in a different context and by a different method.
- [41] The numerical search is more difficult than in the case of a single solution.
- [42] Note that the additional noise source does not need necessarily be of a thermal origin. In SQUIDS, for example, it could be an external magnetic flux noise.
- [43] Our qualitative analysis indicates that, in addition, some new features may appear in the multi-well case, but this has not yet been studied in detail.
- [44] For the sake of brevity, we refer to region 3 as an “at-

- tractor” too.
- [45] Freidlin, M.I. and Wentzell, A.D., *Random Perturbations in Dynamical Systems* (Springer Verlag, New York, 1984).
- [46] R. Ferrando, R. Spadacini, G.E. Tommei, “Kramers problem in periodic potentials: Jump rate and jump lengths”, *Phys. Rev. E* **48**, 2437 (1993).
- [47] Some of the results [32] are closely related to some results of [35] which were obtained by a different method and in a different context.
- [48] M.I. Dykman, M.M. Millonas, V.N. Smelyanskiy, “Observable and hidden singular features of large fluctuations in nonequilibrium systems”, *Phys. Lett. A* **195**, 53 (1994).
- [49] In “long” jumps in a multi-barrier potential with equal or nearly equal barriers, a monotonic exponential dependence on friction was found in earlier works (see e.g. [46] and [3] respectively). However, the obvious reason that oscillations and cusps were not found in those studies is that they can only arise in the case of distinctly different barriers levels.
- [50] Note however that pre-exponential time-scales in other systems (e.g. in SQUIDS or NEMS/MEMS6) may be much smaller, so that the relevant flux may be readily simulated and/or measured.
- [51] H. Risken, *The Fokker-Planck Equation*, 2nd ed. (Springer-Verlag, Berlin, 1992).
- [52] B. Hille, *Ionic Channels of Excitable Membranes* (Sinauer Associates Inc., Sunderland, 1992).
- [53] J. Zheng and M.C. Trudeau, *Handbook of Ion Channels* (CRS Press, 2015).
- [54] I.K. Kaufman, P.V.E. McClintock, R.S. Eisenberg, “Coulomb blockade model of permeation and selectivity in biological ion channels”, *New J. Phys.* **17**, 083021 (2015).
- [55] M. von Haartman and M. Östling, *LOW-FREQUENCY NOISE IN ADVANCED MOS DEVICES* (Springer, 2007).
- [56] H.B. Chan, private communication.
- [57] S.M. Soskin, T.L. Linnik, unpublished.
- [58] J. Moser, J. Güttinger, A. Eichler, et al., “Ultrasensitive force detection with a nanotube mechanical resonator”, *Nature Nanotechnology* **8**, 493 (2013).
- [59] S.O. Erbil, U. Hatipoglu, C. Yanik, M. Ghavami, A.B. Ari, M. Yuksel, and M.S. Hanay, “Full Electrostatic Control of Nanomechanical Buckling”, *Phys. Rev. Lett.* **124**, 046101 (2020).